Original Article Open Access

Archives Of Breast Cancer

DOI: 10.32768/abc.2023102187-199

Cholesterol *de novo* Biosynthesis in Paired Samples of Breast Cancer and Adjacent Histologically Normal Tissue: Association with Proliferation Index, Tumor Grade, and Recurrence-Free Survival

Danila Coradini[§*a], Federico Ambrogi[a,b], Gabriele Infante[§a,c]

[a]*Laboratory of Medical Statistics and Biometry, Department of Clinical Sciences and Community Health, Campus Cascina Rosa, University of Milan, Italy*

[b]*Scientific Directorate, IRCCS Policlinico San Donato, San Donato Milanese, Italy*

[c]*Clinical Epidemiology and Trial Organization Unit, Department of Applied Research and Technological Development, Fondazione IRCCS Istituto Nazionale Tumori, Milan, Italy*

[§]Authors with the same contribution

ARTICLE INFO

Received:
29 December 2022
Revised:
10 March 2023
Accepted:
11 March 2023

Keywords:
Breast Neoplasm,
Cholesterol/biosynthesis,
Gene Expression,
Neoplasm Grading,
Event-Free Survival

ABSTRACT

Background: Cholesterol is an essential component of cell membranes whose local *de novo* biosynthesis may occur in response to additional cellular requirements, especially cell proliferation. In this study, we investigated: (1) the differential expression of the genes coding for the main enzymes involved in cholesterol biosynthesis (*ACAT2*, *HMGCS1*, *HMGCR*, *FDFT1*, *SQLE*, *LSS*, and *NSDHL*), or the proteins that control their activity (*SREBF2*, *SCAP*, and *INSIG1*), in patient-matched samples of breast cancer and adjacent histologically normal (HN) tissue; (2) their association with the expression of *MKI67* or the histologic tumor grade (in particular, G2); (3) their association with recurrence-free survival (RFS).

Methods: Nonparametric rank-based models for longitudinal data were applied to assess the differential gene expression between the tumor and the adjacent HN tissue from the same patient or between the classes of tumor grade. Spearman's rank correlation and Cox proportional hazard models were used to assess the correlation between the genes and their association with RFS.

Results: Compared to the adjacent HN tissue, *HMGCS1*, *HMGCR*, *SQLE*, and *NSDHL* genes were more expressed in the tumor. Their expression progressively increased according to tumor grade and correlated positively with *MKI67*. *ACAT2*, *HMGCR*, and *NSDHL* genes were associated with a high risk of recurrence even when adjusted for age, tumor grade, or immunohistochemical Ki67.

Conclusion: The findings indicated that some genes involved in cholesterol biosynthesis were more expressed in cancerous tissue, correlated positively with tumor grade and *MKI67* expression, and were associated with RFS, thus substantiating the relationship between *de novo* cholesterol biosynthesis and tumor aggressiveness.

***Address for correspondence:**
Danila Coradini, MD
Department of Clinical Sciences and Community Health, University of Milan, Via Vanzetti 5, 20133, Milan, Italy.
Tel: +223902065
Fax: +250320866
Email: danila.coradini@gmail.com

INTRODUCTION

Cell proliferation is a hallmark of many solid tumors, including breast cancer, and is frequently associated with cell morphology disruption.[1] Consequently, evaluating the proliferative activity of the tumor and describing how abnormal the tumor tissue looks compared with the corresponding normal

tissue is essential to characterizing a newly diagnosed tumor and predict patient's outcome.

Among the methods used to evaluate cell proliferation and determine the so-called proliferation index, the immunohistochemical detection of Ki-67 − the nuclear antigen coded by the *MKI67* gene − is the most widely applied.[2-5] The choice is based on the evidence that, although the functional significance of Ki-67 remains unclear, the protein is preferentially present in proliferating cells during all active phases of the cell cycle but absent in resting cells, making it an excellent marker for determining the growth fraction of a given cell population.[6]

Likewise, the histological tumor grade is an essential prognostic factor because it describes tissue alterations and predicts how a tumor is likely to grow and spread.[7] Accordingly, breast tumors are classified as: "low grade or predominantly well-differentiated" (grade 1, G1), when the tissue organization looks similar to the normal tissue, and growth and spread are slow; "high grade or poorly differentiated" (grade 3, G3), when they have abnormal-looking cells and tend to grow and spread fast; "intermediate-grade or moderately differentiated" (grade 2, G2), when they show an intermediate and highly variable state in morphology.[8]

Usually, G1-tumors are associated with a null/weak Ki-67 staining and a better prognosis, whereas G3-tumors that grow and spread more quickly are often associated with a strong Ki-67 staining and an unfavorable prognosis. In the middle, there is the heterogeneous subgroup of G2-tumors that accounts for about 30–60% of diagnosed breast cancers, where the association with Ki-67 staining is variable and prognosis less predictable. Because of this heterogeneity, patients with a G2-tumor often do not receive the most appropriate treatment.[9]

Proliferative activity is associated with cell duplication. Consequently, proliferating cells require additional cholesterol, the main component of all cell membranes. Tumor cells satisfy this requirement by implementing *de novo* cholesterol biosynthesis. As depicted in Figure 1, cholesterol biosynthesis is a complex process including a series of enzymes that, which starts from the condensation of two molecules of acetyl-coenzyme A (acetyl-CoA) and through the mevalonate pathway. Cholesterol biosynthesis is regulated by sterol regulatory element-binding protein (SREBP), a transcription factor that, under cholesterol-deprivation conditions, promotes the expression of several genes including *HMGCR* and *SQLE*, which code, respectively, for HMG-CoA reductase (the recognized first rate-limiting enzyme) and squalene epoxidase (the first committed step of cholesterol biosynthesis).

Cumulating evidence has indicated that, in cancer cells, this transcriptional control is often lost, SREBP is overexpressed, and intracellular accumulation of cholesterol occurs.[10]

This dysregulation of cholesterol metabolism plays a crucial role in malignant transformation and tumor progression.[11-13] Therefore, in this study, we investigated: (1) the differential expression of the genes coding for the main enzymes involved in cholesterol biosynthesis (*ACAT2*, *HMGCS1*, *HMGCR*, *FDFT1*, *SQLE*, *LSS*, and *NSDHL*), or the proteins that control their activity (*SREBF2*, *SCAP*, and *INSIG1*), in patient-matched samples of breast cancer and adjacent histologically normal (HN) tissue; (2) their association with the expression of *MKI67* or the histologic tumor grade (in particular G2); (3) their association with recurrence-free survival (RFS).

METHODS

The study was performed using a publicly accessible dataset from the NCBI Gene Expression Omnibus (GEO) database (HTTPS://www.ncbi.nlm.nhi.gov/geo/) and identified by the GEO accession number GSE93601. As described in the original articles,[14-16] the dataset consisted of 194 paired formalin-fixed paraffin-embedded (FFPE) breast cancer and adjacent histologically normal tissues from women (the Nurses' Health Study (NHS) cohort) who developed invasive breast cancer during a prospective study aimed at evaluating alcohol consumption and risk of breast cancer.

The Human Subjects Committee at Partners Healthcare System and Brigham and Women's Hospital in Boston, MA, approved the original study. All patients consented to provide excess tissues for research purposes.

As described in the original article,[14] tumor samples were classified according to the molecular subtype by tissue microarray analysis (TMA) using a panel of immunohistochemical markers (ER, PR, HER2, CK 5/6, EGFR). TMA was performed on three cores for each patient, and a tumor was classified as positive if there was staining in any of the three cores and negative if no immunostaining was present. Tumor cells that showed any nuclear staining for estrogen (ER) or progesterone receptor (PR) (≥1%) were considered ER-positive or PR-positive; therefore, low ER-positive or PR-positive (1 to 10% of tumor cell nuclei staining) and ER-positive or PR-positive (>10% of tumor cell nuclei staining) were all categorized as positive.

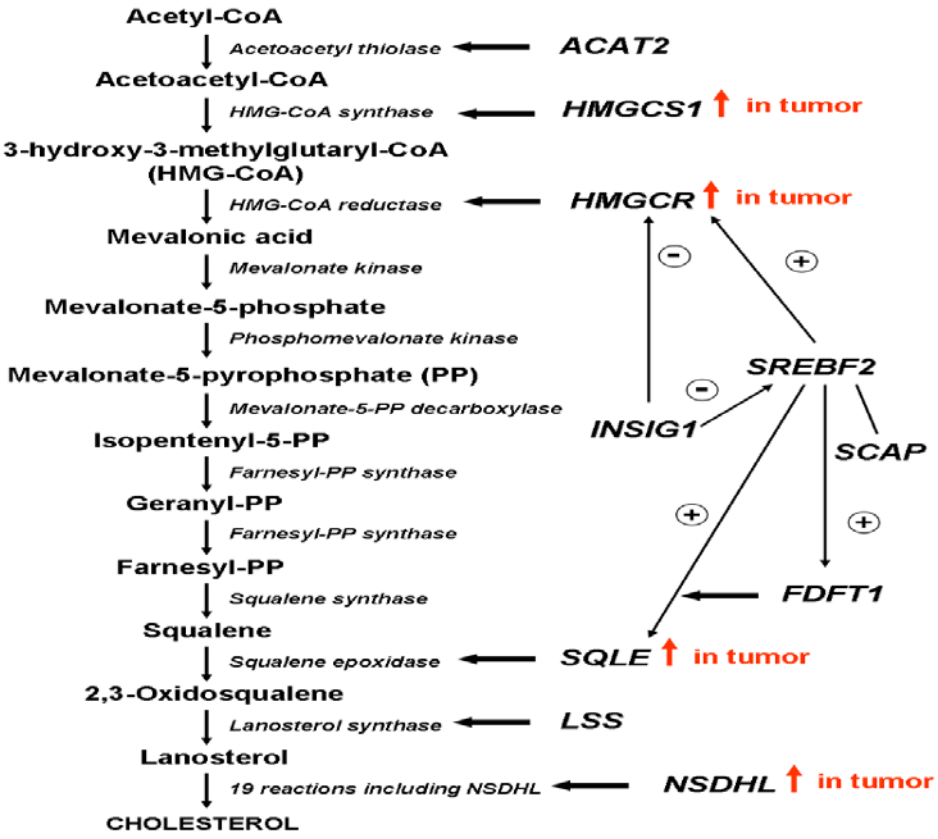

Figure 1. Schematic diagram depicting the genes encoding the enzymes involved in cholesterol biosynthesis or the proteins that control their activity. The process starts from the condensation of two molecules of acetyl-coenzyme A (acetyl-CoA) by the acetoaceyl thiolase (encoded by *ACAT2*), the synthesis of HMG-CoA by the HMG-CoA synthase (encoded by *HMGCS1*), and its reduction to mevalonic acid by the HMG-CoA reductase (encoded by *HMGCR*) which enters the mevalonate pathway bringing to cholesterol. Cholesterol biosynthesis is regulated by sterol regulatory element-binding protein (SREBP) transcription factor. In the presence of cholesterol, the SREBP precursor is retained in the endoplasmic reticulum (ER) by a tight association with the cholesterol-sensing SREBP cleavage-activating protein (SCAP), which, in turn, binds reversibly another ER-resident membrane protein, the insulin-induced gene (INSIG). Binding to both INSIG and SCAP, cholesterol mediates the formation of the ternary complex. Conversely, under cholesterol-deprivation conditions, the binding between INSIG and SCAP disrupts, and SCAP undergoes a conformational change that unmasks the ER-export signal that allows the transport of the SCAP-SREBP complex to the Golgi apparatus. Here, SREBP is proteolytically cleaved. Then, the mature form of the transcription factor is released in the cytoplasm, migrates to the nucleus where activates the transcription of several genes including *HMGCR*, *FDFT1* and *SQLE*. *ACAT2*: Acetyl-CoA Acetyltransferase 2; *FDFT1*: Farnesyl-Diphosphate Farnesyltransferase 1; *HMGCR*: HMG-CoA reductase; *HMGCS1*: HMG-CoA synthase 1; *INSIG1*: Insulin-induced gene 1; *LSS*: Lanosterol synthase; *NSDHL*: NAD(P) Dependent Steroid Dehydrogenase-Like; *SCAP*: SREBP cleavage-activating protein; *SQLE*: Squalene Epoxidase; *SREBF2*: Sterol regulatory element-binding transcription factor 2.

Tumor cells were considered positive for HER2 protein overexpression when more than 10% of the cells showed moderate or strong membrane staining (2+ and 3+). Tumors were considered CK-positive or EGFR-positive if any cytoplasmic and/or membranous staining was detected in the tumor cells. Tumors that were ER-positive and/or PR-positive, and HER2-negative were classified as luminal A; tumors that were ER-positive and/or PR-positive, and HER2-positive were classified as luminal B; tumors that were ER-negative, PR-negative, and HER2-positive were classified as HER2-enriched; and tumors that were negative for ER, PR, and HER2, and positive for CK 5/6 and/or EGFR were classified as basal-like. Tumors lacking expression of all five markers were considered unclassified.

Of the 194 tumors selected for our study, with an available immunohistochemical evaluation of Ki-67, 86 (44%) were luminal A, 69 (36%) were luminal B, 12 (6%) were HER2-enriched, 20 (10%) were basal-like, and 7 (4%) were unclassified.

In addition to the transcriptome, the dataset provided information about the tumor size, the histological grade of the tumor, the immunohistochemical evaluation of ER, PR, HER2 and Ki-67 status (all expressed as positive and negative), and the recurrence-free survival (RFS), defined as the time from diagnosis to reported breast cancer recurrence (Table 1).

Table 1. Patients and tumors characteristics

Characteristics		N (%)
Age, years		
Mean (range)	65 (38 – 81)	
Tumor size		
T1-T2		131 (68.9)
T3		48 (25.3)
T4		11 (5.8)
Not Available		4
Tumor grade		
1: Predominantly well-differentiated		43 (22.6)
2: Moderately differentiated		100 (52.7)
3: Poorly differentiated		47 (24.7)
Not Available		4
Tumor ER (IHC)		
Negative		37 (19.2)
Positive		156 (80.8)
Not Available		1
Tumor PR (IHC)		
Negative		37 (19.2)
Positive		156 (80.8)
Not Available		1
Tumor HER2 (IHC)		
Negative		130 (67.7)
Positive		62 (32.3)
Not Available		2
Tumor Ki-67 (IHC)		
Negative		143 (73.7)
Positive		51 (26.3)
Recurrence		
Negative		158 (81.4)
Positive		36 (18.6)
Recurrence-Free Survival, months		
Median (range)	198.5 (2.5 – 476)	

Gene expression estimates were obtained using the [hGlue_3_0] Custom Affymetrix Human Transcriptome Array platform (GEO accession GPL22920), filtered, and $\log_2$ transformed.

Statistical analysis

To assess the differential gene expression between tumor and adjacent HN tissue from the same patient and between the classes of tumor grade, nonparametric rank-based models for longitudinal data[17] were applied. In particular, the F1-LD-F1 (factor 1 – longitudinal data – factor 1) design was chosen, with tissue type (HN or tumor) as a sub-plot factor and tumor grade as a whole-plot factor. A sub-plot factor is a factor in which the response variable is recorded according to its categories for each subject, whereas a whole-plot factor is a factor effective for each subject independently of the sub-plot factor. This model is suitable for non-Gaussian-distributed variables, robust to outliers, indifferent to heteroscedasticity, and does not rely on parametric assumptions. The gene expression values were replaced with their overall ranks, and the relative effects, which could serve as effect size measures, were estimated as a function of the data's cumulative distribution and ranged between 0 and 1. A modified-ANOVA-type test was used to test the hypotheses of no main effect of the type of tissue, tumor grade, and no interaction between tissue type and tumor grade.[18] The results were graphically depicted, showing the estimates of the relative effect between HN and tumor tissue.

The Wilcoxon-Signed-Rank test for paired data was used to assess the differential gene expression between the tissue types in a given class of tumor grade. The resulting P-values were adjusted for multiple testing using Benjamini–Hochberg (BH) method. In the same way, the unpaired Wilcoxon-Mann-Whitney test with BH correction was used to assess the differential gene expression between pair tumor grade levels according to tissue type.

For each gene, the univariate Cox proportional hazard model for RFS outcome was fitted with gene expression modeled as a 3-knot restricted cubic spline. If the non-linear spline component resulted in a P-value >0.1 at the Wald test, the gene expression

was included in the model as linear. Moreover, two different multivariable Cox models were fitted for each gene: one added age and tumor grade as the covariate, and the other added age and the binary immunohistochemical evaluation of Ki-67 protein staining. In multivariable modeling, the empirical 1-in-10 rule has been considered. By the Cox model, the hazard ratio (HR) of each gene expression with 95% confidence interval (95% CI) and the Wald P-value was obtained. For the genes added as linear, the HR references were 75th versus 25th percentile of gene expression, while for the genes modeled as spline, HR references were 25th percentile versus median and 75th percentile versus median.

Spearman's rank correlation rho was used to investigate the correlation among genes in the HN or tumor tissue. All P-values were adjusted for multiple testing using the BH method. Analyses were performed using the open-source software R, version 4.1.1. (http://www.R-project.org).

RESULTS

Expression of the genes involved in the cholesterol biosynthesis in cancerous and HN tissue, and association with tumor grade

Paired-samples analysis showed that, while for *ACAT2*, *FDFT1*, and *LSS*, there was no evidence of differential expression in tumor and adjacent HN tissue and among the classes of tumor grade (Supplementary Figure 1), *HMGCS1*, *HMGCR*, *SQLE*, and *NSDHL* were more expressed in tumor compared to the HN tissue and positively associated with tumor grade (Figure 2). It is noteworthy that the differential expression between HN and tumor was statistically significant in G2 and G3 subgroup but not in the G1 subgroup (Figure 2 panels C).

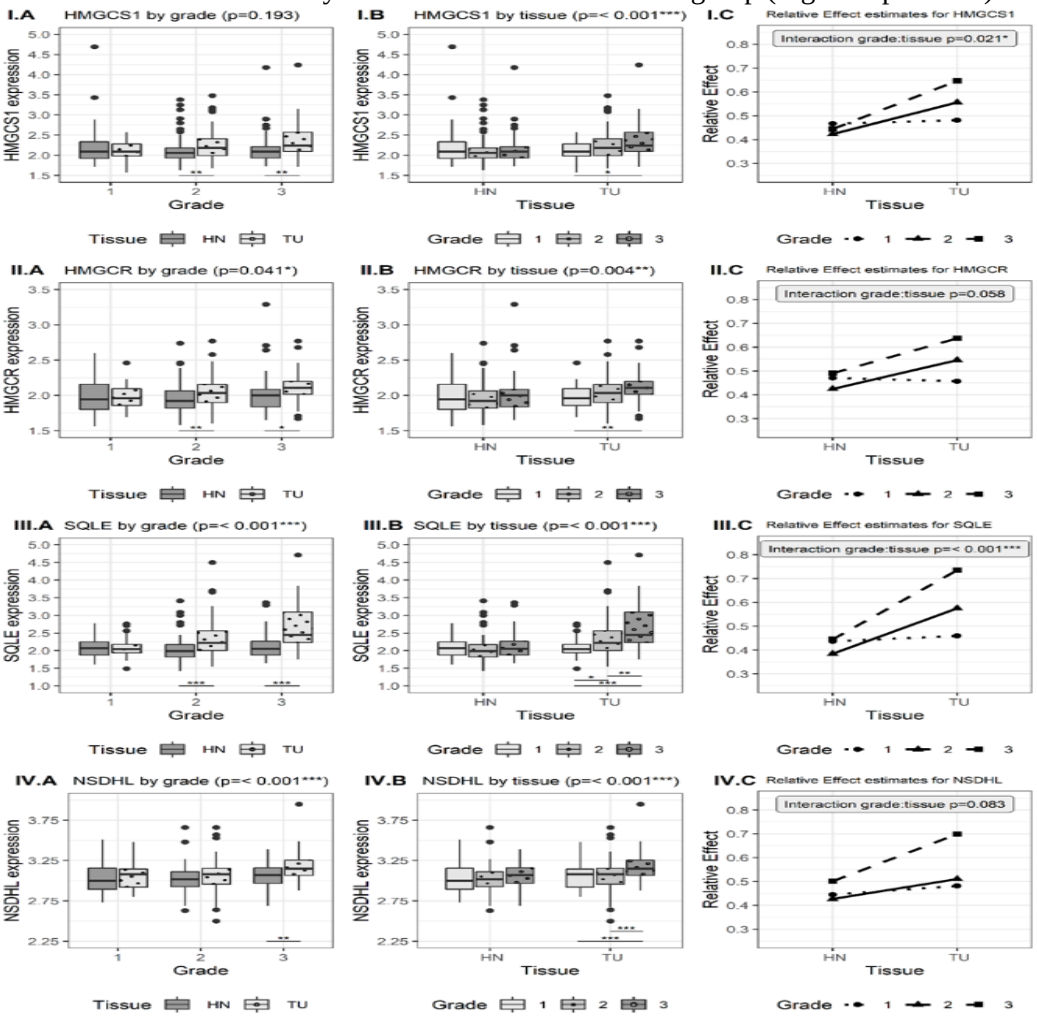

Figure 2. Expression of *HMGCS1* (I), *HMGCR* (II), *SQLE* (III), and *NSDHL* (IV) gene in paired samples of histologically normal (HN) and cancerous tissue (TU) from patients with breast cancer according to tumor grade (G1, G2, G3) and model estimates. In panel **A,** boxplots compare the gene expression in HN and TU tissue according to the tumor grade. In panel **B,** boxplots compare the gene expression in G1, G2, and G3 subgroups according to the tissue. Panel **C** shows the interaction between tumor grade and tissue. The nonparametric rank-based model with the F1-LD-F1 design was chosen, with tissue type (HN or tumor) as a sub-plot factor and tumor grade as a whole-plot factor (see details in the Statistical analysis section).

Concerning the genes that regulate cholesterol biosynthesis, the expression level of *SREBF2* and *INSIG1* was higher in the tumor than in the adjacent HN tissue and increased along with tumor grade. Conversely, there was no evidence of differential expression of *SCAP* between HN and cancerous tissue and among tumor grade subgroups (Figure 3).

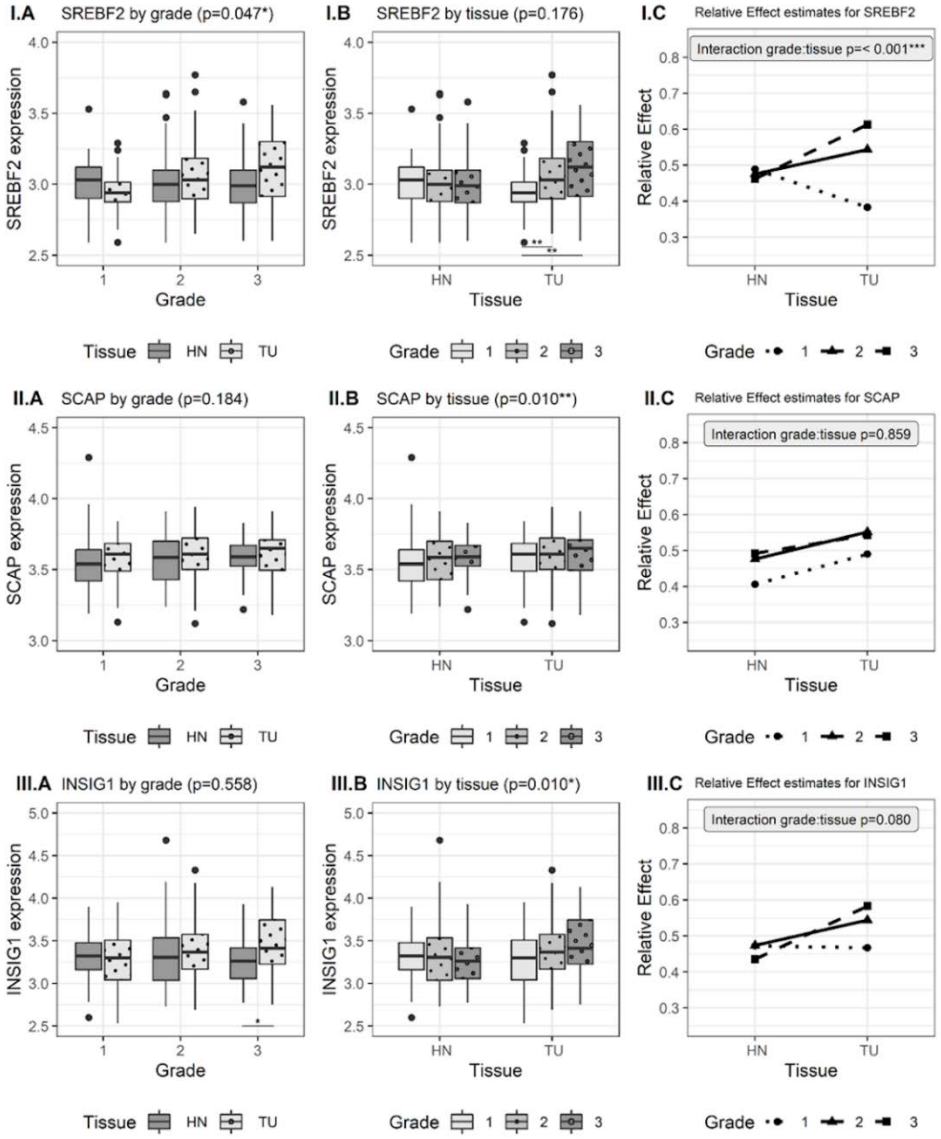

Figure 3. Expression of *SREBF2* (I), *SCAP* (II), and *INSIG1* (III) gene in paired samples of histologically normal (HN) and cancerous tissue (TU) from patients with breast cancer according to tumor grade (G1, G2, G3) and model estimates. In panel **A,** boxplots compare the gene expression in HN and TU tissue according to the tumor grade. In panel **B,** boxplots compare the gene expression in G1, G2, and G3 subgroups according to the tissue. Panel **C** shows the interaction between tumor grade and tissue. The nonparametric rank-based model with the F1-LD-F1 design was chosen, with tissue type (HN or tumor) as a sub-plot factor and tumor grade as a whole-plot factor (see details in the Statistical analysis section).

As expected, the expression level of *MKI67* was higher in the tumor than in the adjacent HN tissue, and the median expression level of *MKI67* considerably increased according to tumor grade (Supplementary Figure 2), in agreement with the progressive increase in the percentage of Ki-67-positive cases, as assessed by immunohistochemistry. In G2 and G3 subgroups, Ki-67-positive tumors had a significantly higher median level of *MKI67* expression compared to Ki-67-negative tumors. Statistical analyses performed on the subgroup of the ER-positive tumors did not show substantial differences from those of the overall cases series (data not shown).

Effect of the association of genes involved in the cholesterol biosynthesis and MKI67 on recurrence-free survival

Table 2 shows the association of gene expression with RFS. Each gene maintained an association with RFS similar to the univariable estimate after

adjustment for age and tumor grade or age and immunohistochemical Ki-67. In particular, *ACAT2* (HR: 1.62, 95%CI: 1.14-2.32, P=0.009) and *HMGCR* (HR:1.62, 95% CI:1.10-2.37, P=0.014) showed a higher and statistically significant association with RFS in the univariable analysis which persisted in the multivariable analysis when tumor grade or Ki-67 was included.

Figure 4 shows the graphical representation of the log relative hazard as a function of gene expression adjusted for age and Ki-67 immunohistochemical evaluation (Table 2).

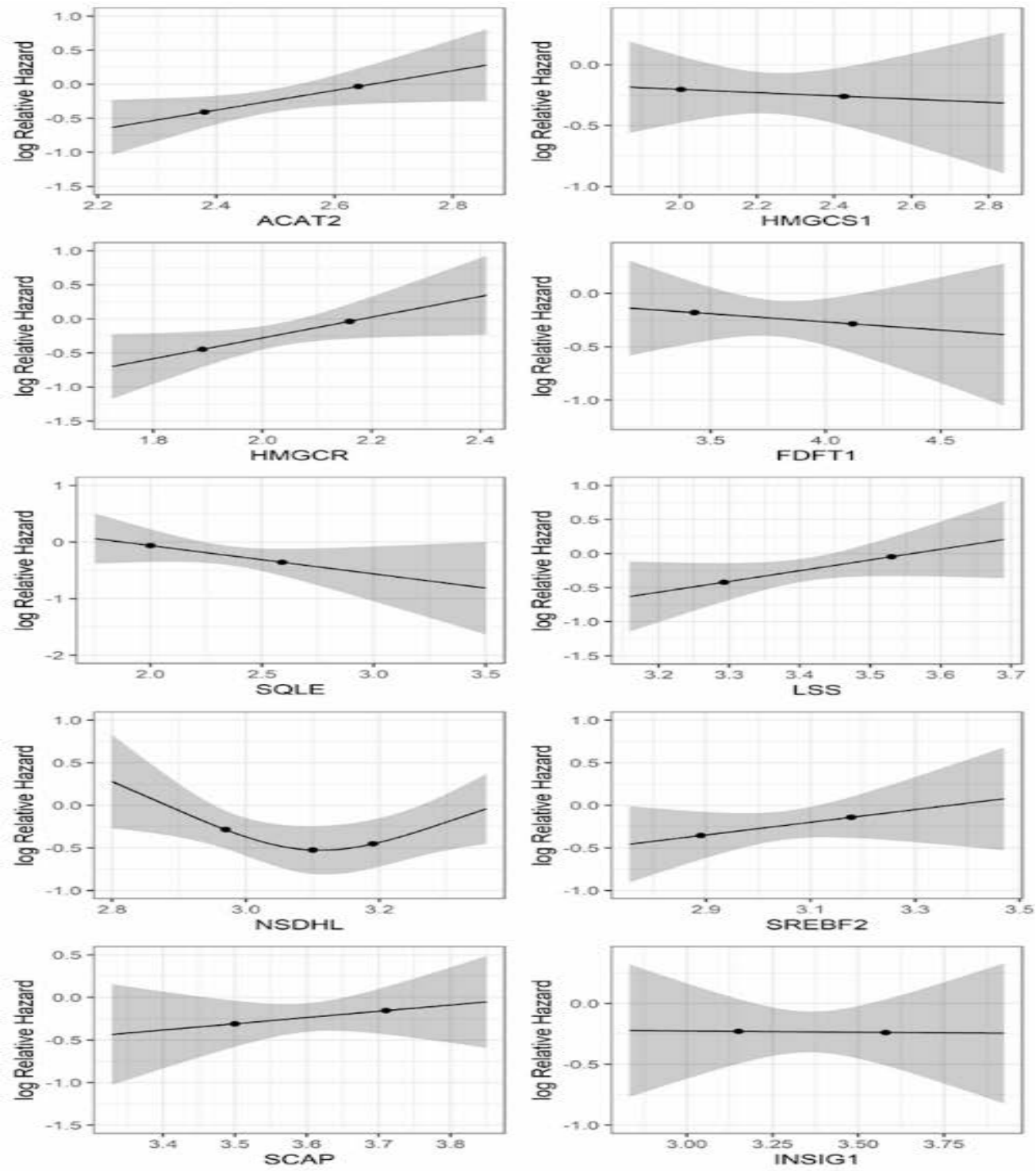

Figure 4. Log Relative Hazard estimates and corresponding pointwise 95% confidence intervals from immunohistochemical Ki67-adjusted Cox Proportional Hazard models. Points represent the 25th and the 75th percentiles of the gene expression distribution. For the *NSDHL* gene, which is modeled as restricted cubic spline, points represent the 25th percentile, median, and 75th percentile of the gene expression distribution.

Table 2 Univariable, age-tumor grade-adjusted and age-immunohistochemical Ki67-adjusted Cox Proportional Hazard (PH) model's estimates of recurrence-free survival for genes involved in cholesterol biosynthesis, their regulators, and *MKI67* in overall cases series

			Univariable Cox PH Model		Grade-age-adjusted Cox PH Model		Ki67-age-adjusted Cox PH Model	
	Non-linear term Wald *p*-value	Comparison	HR (95% CI)	Wald *p*-value	HR (95% CI)	Wald *p*-value	HR (95% CI)	Wald *p*-value
ACAT2	0.905	2.64 *vs.* 2.38	1.62 (1.14-2.32)	0.009**	1.62 (1.13-2.33)	0.009**	1.46 (1.02-2.08)	0.039*
HMGCS1	0.664	2.43 *vs.* 2.00	0.98 (0.66-1.46)	0.937	0.94 (0.62-1.40)	0.748	0.94 (0.64-1.39)	0.765
HMGCR	0.309	2.16 *vs.* 1.89	1.62 (1.10-2.37)	0.014*	1.58 (1.07-2.34)	0.023*	1.51 (1.02-2.24)	0.040*
FDFT1	0.136	4.12 *vs.* 3.43	0.97 (0.62-1.51)	0.877	0.96 (0.61-1.50)	0.844	0.90 (0.57-1.41)	0.632
SQLE	0.925	2.59 *vs.* 2.00	0.81 (0.55-1.19)	0.283	0.75 (0.49-1.13)	0.172	0.74 (0.49-1.12)	0.158
LSS	0.978	3.53 *vs.* 3.29	1.50 (0.94-2.41)	0.087	1.46 (0.91-2.35)	0.113	1.45 (0.92-2.30)	0.111
NSDHL§	0.013*	2.97 *vs.* 3.10 3.19 *vs.* 3.10	1.21 (0.95-1.53) 1.08 (0.95-1.21)	0.042*	1.19 (0.93-1.52) 1.07 (0.94-1.22)	0.061	1.27 (0.99-1.63) 1.08 (0.95-1.22)	0.022*
SREBF2	0.298	3.18 *vs.* 2.89	1.24 (0.83-1.86)	0.300	1.17 (0.76-1.78)	0.478	1.25 (0.83-1.86)	0.285
SCAP	0.590	3.71 *vs.* 3.50	1.18 (0.75-1.85)	0.479	1.14 (0.72-1.79)	0.583	1.17 (0.76-1.81)	0.477
INSIG1	0.834	3.58 *vs.* 3.15	1.03 (0.67-1.59)	0.878	0.98 (0.64-1.53)	0.946	0.99 (0.65-1.52)	0.980
MKI67	0.948	2.85 *vs.* 2.32	1.32 (0.97 -1.78)	0.074	1.37 (0.95-1.97)	0.089		

§Because of a statistically significant non-linear term Wald test *p*-value, restricted cubic spline was used instead of a linear covariate. For linear covariate, the comparison is 75th *vs.* 25th percentile is provided, whereas for restricted cubic spline covariates, 25th *vs.* median and 75th *vs.* median comparisons are reported. Significance at $p < 0.05$ (*) and $p < 0.01$ (**).

While for *ACAT2*, *HMGCR*, *SCAP*, *LSS*, and *SREBF2*, the log relative hazard increased with increasing gene expression, for *SQLE*, *HMGCS1*, and *FDFT1*, the log relative hazard decreased. The flat profile of the *INSIG1* gene indicated a weak association with RFS. *NSDHL* was the only gene with a statistically significant non-linear association with RFS, as indicated by the Wald test on the non-linear spline component in the univariable Cox model (P=0.013). Although the main effect of *NSDHL* on RFS was slightly significant in the univariable analysis (P=0.042) and not significant in the age-tumor grade-adjusted model (P=0.061), the gene showed a statistical significance in the age-Ki-67-adjusted model (P=0.022) with a characteristic U-shape trend in the curve of the log relative hazard as a function of gene expression adjusted for age and immunohistochemical Ki-67. While for values of *NSDHL* gene expression up to the median, the log relative hazard decreased, for gene expression values superior to the median, the log relative hazard increased. No substantial differences were detected in the association of the genes with the RFS in the subgroup of ER-positive tumors compared with the overall cases series (data not shown).

Correlation between the genes involved in cholesterol biosynthesis and MKI67 in cancerous and HN tissue as a function of tumor grade

As shown in Figure 5, in the tumor tissue, only the expression of *SQLE* correlated significantly with that of *MKI67* in all three G subgroups, with a positive degree of correlation that remained relatively stable (G1: r = 0.52, G2: r = 0.43, G3: r = 0.49) whereas *MKI67* correlated significantly and positively with *HMGCS1* (r = 0.39) only in the G2 subgroup and with *ACAT2* (r = 0.45) only in the G3 subgroup. None of these correlations was significant in the corresponding HN tissue.

About the interrelation among the genes involved in cholesterol biosynthesis, we found that the only remarkable differences among the tumors of the three G subgroups were the progressive increase in the positive correlation between *HMGCS1* and *SQLE* (G1: r = 0.03, G2: r = 0.52, G3: r = 0.60) and between *HMGCR* and *FDFT1* (G1: r = 0.18, G2: r = 0.48, G3: r = 0.62). Similar to the G1-tumors, in HN tissues, there was no evidence of correlation. Conversely, HN tissue showed a progressive decrease in the positive correlation between *SREBF2* and *SCAP* among the classes of tumor grade (G1: r = 0.49, G2: r = 0.37, G3: r = 0.02).

DISCUSSION

The results of the present study indicate that, compared to the adjacent HN tissue, tumors show an increased expression of the majority of the genes coding for the enzymes involved in the *de novo* biosynthesis of cholesterol or the proteins that regulate their activity. In particular, *HMGCS1*, *HMGCR*, *SQLE*, and *NSDHL* showed a progressive increase in their expression level according to tumor grade and a positive correlation with the expression of *MKI67*, in agreement with the growing body of literature showing a relationship between *de novo* cholesterol production and tumor aggressiveness, suggesting that the dysregulation of the mevalonate pathway promotes the development and progression of several solid tumors including breast cancer.[11-13] Indeed, HMG-CoA synthase (coded by *HMGCS1*) is emerging as the mediator of cancer stem cell enrichment in luminal and basal models of breast cancer,[19] MG-CoA reductase and squalene epoxidase (coded by *HMGCR* and *SQLE*, respectively) are recognized as the first rate-limiting enzyme and the first committed step of cholesterol biosynthesis,[20] and NAD(P)-dependent steroid dehydrogenase-like (coded by *NSDHL*) has recently been associated with an unfavorable prognosis and metastatic spread.[21,22]

However, the results also indicate that while high expression levels of *HMGCR* and *NSDHL* were associated with an increased risk of recurrence, even when adjusted for tumor grade and immunohistochemical Ki-67, the expression levels of *HMGCS1* and *SQLE* did not. Furthermore, the findings indicated that the high risk of recurrence was associated both with low and high levels of *NSDHL* expression. Although remarkable, the finding needs confirmation in other independent case series before advancing any biological explanation and drawing clinical conclusions.

Another interesting finding is that, despite lacking a differential expression between cancerous and HN tissue, *ACAT2* expression was significantly associated with the risk of recurrence even when adjusted for tumor grade and immunohistochemical Ki67. Patients with high expression levels of *ACAT2* had an increased risk of recurrence (HR = 1.62) compared to patients with low expression levels. To explain this apparent contradiction, we must consider the mechanism of action of this enzyme. Usually, the Acetyl-CoA acetyltransferase 2 is present in the cytoplasm of normal cells as an inactive monomer. In response to a proliferative stimulus, like that induced by the epidermal growth factor (EGF), the enzyme is converted to an active tetrameric form by the tyrosine residue of the intracellular domain of the EGR receptor (EGFR), phosphorylated after the binding with the growth factor. Once activated, Acetyl-CoA acetyltransferase 2 catalyzes the formation of acetoacetyl-CoA from two molecules of acetyl-CoA and starts the biosynthesis of cholesterol. In cancer

cells, where the *EGFR* gene is frequently overexpressed, this mechanism prevales, and cholesterol accumulation occurs. In line with this explanation is the increased correlation between *ACAT2* and *EGFR* in tumors compared to HN tissue (r = 0.43 *vs*. r = 0.36) and the positive correlation between *ACAT2* and *MKI67*.

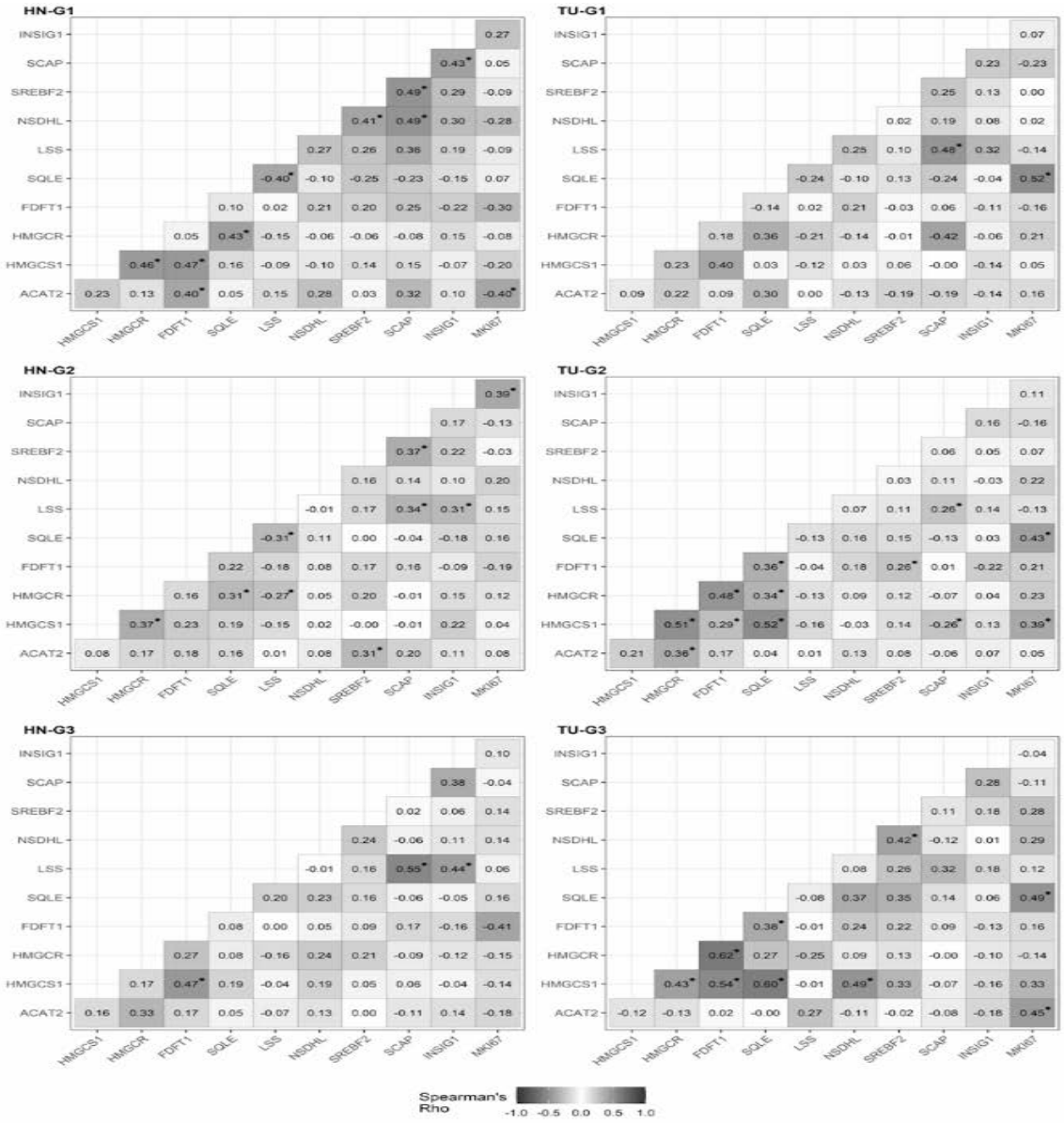

Figure 5. Correlation matrix among the genes involved in cholesterol biosynthesis, their regulators, and *MKI67* in histologically normal (HN) and cancerous (TU) tissue. Upper panels refer to the overall cases series, and lower panels refer to the G2 subgroup. Spearman's Rho correlation coefficients are reported: the darker the cell, the higher the correlation coefficient. Star indicates a p-value < 0.05 after the adjustment for multiple testing correlation.

Concerning the genes coding for the proteins that control cholesterol biosynthesis, the finding that the expression of *SREBF2* was significantly higher in tumor than in the adjacent HN tissue, positively associated with tumor grade, and correlated with *MKI67*, is not surprising considering the role played by SREBP in the transcription of *HMGCR* and *SQLE* genes. Conversely, the high expression level of *INSIG1* in the tumor, its association with tumor grade, and the positive correlation with *MKI67* were almost unexpected, especially considering that INSIG is the negative regulator of the SREBP-dependent transcriptional activity.[23] Indeed, under cholesterol-deprivation conditions, like those occurring in actively proliferating tumor cells, the cholesterol-mediated binding of INSIG with SCAP disrupts, and the SCAP-SREBP complex moves to the Golgi complex, where the SREBP precursor is processed to enter the nucleus and activate the transcription of several genes including *HMGCR* and *SQLE*. One possible explanation is that, as the proliferative activity increases, tumor cells respond by increasing

the expression of *INSIG1* to restore control over gene transcription and block the production of the cholesterol necessary to assemble new membranes.

Concerning the association between gene expression and RFS, the most remarkable result is that *ACAT2*, *HMGCR*, and *NSDHL* retained their prognosticator capability even when adjusted for Ki67 or tumor grade (Table 2 and Figure 4). The finding has clinical relevance because about 40–60% of the diagnosed breast cancers fall in the heterogeneous class of G2-tumors, characterized by a highly variable morphology, unpredictable risk of distant metastasis recurrence,[8] and possible inadequate treatment.[9] Hence, evaluating the expression profile of the genes involved in *de novo* cholesterol biosynthesis could refine the classification of G2-tumors and consequently improve the patient's prognosis.

In this respect, some recent findings[24] are of great interest because they indicate that the mevalonate pathway may interplay with the Hippo signaling pathway, which plays a pivotal role in the tissue renewal and regeneration by sensing cell density information, controlling the amplification of tissue-specific progenitor cells and promoting apoptosis.[25] The core of the Hippo signaling pathway is a kinase cascade resulting in the phosphorylation and functional inactivation of Yes-associated protein 1 (YAP) and Transcriptional coactivator with PDZ-binding motif (TAZ), two nuclear effectors encoded by *YAP1* and *WWTR1* gene, respectively.[26] While in the presence of high cell density, YAP and TAZ accumulate in the cytoplasm after phosphorylation, in the presence of low cell density, they translocate into the nucleus and act as coregulators in the expression of the genes involved in cell proliferation, death, and migration.[27] Increasing evidence indicates that ectopic expression of YAP/TAZ might stimulate cell proliferation, reduce cell contact inhibition and promote oncogenic transformation and epithelial-mesenchymal transition triggering tumor initiation and metastatic spread.[26]

In their study, Sorrentino et al.[24] have demonstrated that, in *Drosophila melanogaster*, the inhibition of HMG-CoA reductase by statins counteracted the YAP/TAZ nuclear accumulation and the following transcriptional activity. Besides, they proposed a mechanistic model according to which the geranyl-pyrophosphate, produced by the mevalonate cascade, activates Rho GTPases that, in turn, activate YAP/TAZ by inhibiting their phosphorylation and promoting the nuclear accumulation. Furthermore, they showed that, in tumor cells, YAP/TAZ activation is triggered by increased levels of mevalonic acid due to the SREBP transcriptional activity in the gene coding for HMG-CoA reductase.

In agreement with the role of these genes in controlling cell proliferation, the present results show that the expression of *YAP1* and *WWRT1* negatively correlated with that of *MKI67* in HN breast tissue (Supplementary Table 1). Conversely, in the tumor, the negative correlation between Y*AP1* and *MKI67* was retained only in the G1-subgroup, whereas all other correlations disappeared. Since *YAP1* expression did not change in tumor samples compared to the corresponding HN tissue (Supplementary Figure 3), we could hypothesize an activation and nuclear accumulation of YAP protein rather than an increased *YAP1* transcription.

Regarding the correlation between *YAP1* or *WWRT1* and the genes involved in cholesterol biosynthesis, the most remarkable finding is the progressive decrease in the positive correlation of *YAP1* with *FDFT1* in the tumor (G1: $r = 0.68$, G2: $r = 0.52$, G3: $r = 0.47$, Supplementary Table 1). The protein encoded by *FDFT1* gene, farnesyltransferase, is a committed enzyme in cholesterol biosynthesis and catalyzes the dimerization of two molecules of farnesyl-diphosphate to form squalene (Figure 1). According to a negative feedback, the farnesyl-diphosphate converted to squalene cannot be reconverted to geranyl-pyrophosphate, activates Rho GTPases and inhibits YAP/TAZ phosphorylation, suggesting a protective role of *FDFT1* as indicated by the decrease in the HR with increasing levels of *FDFT1* expression (Figure 4). Besides, the decrease in the positive correlation at increasing grade of tumor suggests the progressive disruption of this negative feedback, which results in the YAP/TAZ nuclear accumulation and activation.

CONCLUSION

The findings indicated that some genes involved in cholesterol biosynthesis were more expressed in cancerous tissue, correlated positively with tumor grade and *MKI67* expression, and were associated with RFS, thus substantiating the relationship between *de novo* cholesterol biosynthesis and tumor aggressiveness. Although the results need confirmation in an independent case series, they open new insights on the impact of *de novo* cholesterol biosynthesis on tumor progression and the possibility of exploiting it as a therapeutic target, especially in the problematic class of moderately differentiated breast cancers, whose treatment management remains a debated clinical point, centered on the question of how to avoid the under-treatment with ineffective endocrine therapy and the over-treatment with often unnecessary chemotherapy?

FUNDING

This research did not receive any specific grant from funding agencies in the public, commercial or not-for-profit sectors.

DATA AVAILABILITY

The study was performed using a publicly accessible dataset from the NCBI Gene Expression Omnibus (GEO) database (HTTPS://www.ncbi.nlm.nhi.gov/geo/) and identified by the GEO accession number GSE93601.

CONFLICT OF INTERESTS

The authors have no conflict of interest to declare.

REFERENCES

1. Hanahan D, Weinberg RA. Hallmarks of cancer: the next generation. *Cell*. 2011;144(5):646-674. doi: 10.1016/j.cell.2011.02.013.
2. Allred DC, Harvey JM, Berardo M, Clark GM. Prognostic and predictive factors in breast cancer by immunohistochemical analysis. *Mod Pathol*. 1998;11(2):155-68.
3. Early Breast Cancer Trialists' Collaborative Group. Tamoxifen for early breast cancer: an overview of the randomised trials. *Lancet*. 1998;351(9114):1451-67.
4. Yerushalmi R, Woods R, Ravdin PM, Hayes MM, Gelmon KA. Ki67 in breast cancer: prognostic and predictive potential. *Lancet Oncol*. 2010;11(12):174-83. doi: 10.1016/S1470-2045(09)70262-1.
5. Dowsett M, Nielsen TO, A'Hern R, Bartlett J, Coombes RC, Cuzick J, et al. Assessment of Ki67 in breast cancer: recommendations from the International Ki67 in Breast Cancer Working Group. *J Natl Cancer Inst*. 2011;103(22):1656-64. doi: 10.1093/jnci/djr393.
6. Scholzen T, Gerdes J. The Ki-67 protein: from the known and the unknown. *J Cell Physiol*. 2000;182(3):311-22. doi: 10.1002/(SICI)1097-4652(200003)182:3<311::AID-JCP1>3.0.CO;2-9.
7. Elston CW, Ellis IO. Pathological prognostic factors in breast cancer. I. The value of histological grade in breast cancer: experience from a large study with long-term follow-up. *Histopathology*. 1991;19(5):403-10. doi: 10.1111/j.1365-2559.1991.tb00229.x.
8. Sotiriou C, Wirapati P, Loi S, Harris A, Fox S, Smeds J, et al. Gene expression profiling in breast cancer: understanding the molecular basis of histologic grade to improve prognosis. *J Natl Cancer Inst*. 2006;98(4):262-72. doi: 10.1093/jnci/djj052.
9. Matikas A, Foukakis T, Swain S, Bergh J. Avoiding over- and undertreatment in patients with resected node-positive breast cancer with the use of gene expression signatures: are we there yet? *Ann Oncol*. 2019;30(7):1044-50. doi: 10.1093/annonc/mdz126.
10. Griffiths B, Lewis CA, Bensaad K, Ros S, Zhang Q, Ferber EC, et al. Sterol regulatory element binding protein-dependent regulation of lipid synthesis supports cell survival and tumor growth. *Cancer Metab* 2013;1(1):3. doi: 10.1186/2049-3002-1-3.
11. Clendening JW, Pandyra A, Boutros PC, El Ghamrasni S, Khosravi F, Trentin GA, et al. Dysregulation of the mevalonate pathway promotes transformation. *Proc Natl Acad Sci*. 2010;107(34):15051-6. doi: 10.1073/pnas.0910258107.
12. Llaverias G, Danilo C, Mercier I, Daumer K, Capozza F, Williams TM, et al. Role of cholesterol in the development and progression of breast cancer. *Am J Pathol*. 2011;178(1):402-12. doi: 10.1016/j.ajpath.2010.11.005.
13. Gustbée E, Tryggvadottir H, Markkula A, Simonsson M, Nodin B, Jirström K, et al. Tumor-specific expression of HMG-CoA reductase in a population-based cohort of breast cancer patients. *BMC Clin Pathol*. 2015;15:8. doi: 10.1186/s12907-015-0008-2.
14. Tamimi RM, Baer HJ, Marotti J, Galan M, Galaburda L, Fu Y, et al. Comparison of molecular phenotypes of ductal carcinoma in situ and invasive breast cancer. *Breast Cancer Res*. 2008;10(4):R67. doi: 10.1186/bcr2128.
15. Sisti JS, Collins LC, Beck AH, Tamimi RM, Rosner BA, Eliassen AH. Reproductive risk factors in relation to molecular subtypes of breast cancer: Results from the nurses' health studies. *Int J Cancer*. 2016;138(10):2346-56. doi: 10.1002/ijc.29968.
16. Wang J, Zhang X, Beck AH, Collins LC, Chen WY, Tamim RM, et al. Alcohol Consumption and Risk of Breast Cancer by Tumor Receptor Expression Horm *Cancer*. 2015; 6(0): 237–246. doi: 10.1007/s12672-015-0235-0.
17. Brunner E, Bathke AC, Konietschke F. Two-Factor Crossed Designs. In: Rank and pseudo-rank procedures for independent observations in factorial designs. *Springer International Publishing*. 2018;263-331. doi: 10.1007/978-3-030-02914-2.
18. Brunner E, Dette H, Munk A. Box-type approximations in nonparametric factorial designs. *J Am Stat Ass*. 1997;92(440):1494-502. doi: 10.1080/01621459.1997.10473671.
19. Walsh CA, Akrap N, Garre E, Magnusson Y, Harrison H, Andersson D, et al. The mevalonate precursor enzyme HMGCS1 is a novel marker and key mediator of cancer stem cell enrichment in luminal and basal models of breast cancer. *PLoS One*. 2020;15(7):e0236187. doi: 10.1371/journal.pone.0236187.
20. Gill S, Stevenson J, Kristiana I, Brown AJ. Cholesterol-dependent degradation of squalene monooxygenase, a control point in cholesterol synthesis beyond HMG-CoA reductase. *Cell Metab*. 2011;13(3):260-73. doi: 10.1016/j.cmet.2011.01.015.
21. Yoon SH, Kim HS, Kim RN, Jung SY, Hong BS, Kang EJ, et al. NAD(P)-dependent steroid dehydrogenase-like is involved in breast cancer cell growth and metastasis. *BMC Cancer*. 2020;20(1):375. doi: 10.1186/s12885-020-06840-2.
22. Xue T, Zhang Y, Zhang L, Yao L, Hu X, Xu LX. Proteomic analysis of two metabolic proteins with

potential to translocate to plasma membrane associated with tumor metastasis development and drug targets. *J Proteome Res*. 2013;12(4):1754-63. doi: 10.1021/pr301100r.
23. Yang T, Espenshade PJ, Wright ME, Yabe D, Gong Y, Aebersold R, et al. Crucial step in cholesterol homeostasis: sterols promote binding of SCAP to INSIG-1, a membrane protein that facilitates retention of SREBPs in ER. *Cell*. 2002;110(4):489-500. doi: 10.1016/s0092-8674(02)00872-3.
24. Sorrentino G, Ruggeri N, Specchia V, Cordenonsi M, Mano M, Dupont S, et al. Metabolic control of YAP and TAZ by the mevalonate pathway. *Nat Cell Biol*. 2014;16(4):357-66. doi: 10.1038/ncb2936.
25. Zhao B, Wei X, Li W, Udan RS, Yang Q, Kim J, et al. Inactivation of YAP oncoprotein by the Hippo pathway is involved in cell contact inhibition and tissue growth control. *Genes Dev*. 2007;21(21): 2747-61. doi: 10.1101/gad.1602907.
26. Lei QY, Zhang H, Zhao B, Zha ZY, Bai F, Pei XH, et al. TAZ promotes cell proliferation and epithelial-mesenchymal transition and is inhibited by the hippo pathway. *Mol Cell Biol*. 2008;28(7):2426-36. doi: 10.1128/MCB.01874-07.
27. Hao Y, Chun A, Cheung K, Rashidi B, Yang X. Tumor suppressor LATS1 is a negative regulator of oncogene YAP. *J Biol Chem*. 2008;283(9):5496-5509. doi: 10.1074/jbc.M709037200.

How to Cite This Article

Coradini D, Ambrogi F, Infante G. Cholesterol *de novo* Biosynthesis in Paired Samples of Breast Cancer and Adjacent Histologically Normal Tissue: Association with Proliferation Index, Tumor Grade, and Recurrence-Free Survival. Arch Breast Cancer. 2023; 10(2): 187-99.
Available from: https://www.archbreastcancer.com/index.php/abc/article/view/690